

Mineralogy and Ore Characteristics of the Kujang Pb-Zn Skarn Deposit, Sukabumi Regency, West Java

Eka Harris Suryawan¹, Arifudin Idrus^{*1}, Imam Suyanto², Ilham Ilmawan³, and M. Dzulfikar Faruqi³

¹Department of Geological Engineering, Faculty of Engineering, Universitas Gadjah Mada, Yogyakarta, Indonesia

²Department of Physics, Universitas Gadjah Mada, Yogyakarta

³PT. Generasi Muda Bersatu, Jakarta

Received: September 30, 2022 | Accepted: February 1, 2024 | Published online: April 31, 2024

ABSTRACT. The Kujang Pb-Zn skarn deposit is known to be the newest skarn deposit found in the Sunda-Banda magmatic arc. The skarn orebodies are hosted mainly by limestone, which might be part of the Jampang Formation, where dacite porphyry is interpreted as the ore causative intrusion. Orebodies are mostly found at the contact between marbleized limestone and volcanic rocks and are controlled by NW-SE-trending strike-slip faults. Previous research on the mineralogy and ore characteristics of the Kujang Prospect remains limited to preliminary studies. Using fieldwork data, petrography, ore microscopy, and assay data from core samples, this study aims to characterize the mineralogy of both alteration and ore of the deposit. The alteration of the Kujang Prospect skarn can be divided into 2 phases of alteration, i.e., prograde and retrograde. The occurrence of clinopyroxene, wollastonite, and vesuvianite characterizes the prograde alteration. Garnet is present in very rare amounts. The retrograde alteration is typified by epidote, chlorite, calcite, and actinolite. Metalliferous minerals are represented by sphalerite, galena, pyrrhotite, chalcopyrite, and pyrite. All ore minerals are formed at the early retrograde stage. The deposit's average grade is 2.06 % Pb, 6.45 % Zn, and 1.81 % Cu.

Keywords: Mineralogy and ore characteristics · Skarn deposit · Sukabumi.

1 INTRODUCTION

One kind of deposit enriched with Pb-Zn-bearing minerals and found in almost all metallogenic belts in Indonesia is a skarn deposit (Dana *et al.*, 2019; van Leeuwen, 2018). The existence of the skarn deposit itself is always associated with carbonate-rich rocks that undergo a metamorphism and metasomatism process due to contact with intrusive rock such as those in Erstberg in Papua (Bensaman *et al.*, 2015), Ruwai in Kalimantan (Idrus *et al.*, 2011), and Tuboh in Sumatra (Xu *et al.*, 2021). The Kujang skarn prospect at Sukabumi Regency

is one of the newest economically significant skarn deposits in the Sunda-Banda Arc. The previous research on the Kujang Prospect deposit was limited to a preliminary study and is still unpublished. However, recognizing the mineral and ore characteristics is critically important as a guide for further exploration and mining development of the deposit itself. This study combines petrography, ore microscopy, and assay data from core samples to provide updated and more detailed characterize mineralogy and ore characteristics of the deposit.

2 REGIONAL GEOLOGY

The Kujang Pb-Zn skarn deposit is located in the west part of Java Island. The deposit lies beneath the Early Miocene age Jampang For-

*Corresponding author: A. IDRUS, Department of Geological Engineering, Universitas Gadjah Mada. Jl. Grafika 2 Yogyakarta, Indonesia. E-mail: arifidrus@ugm.ac.id

mation (Figure 1A) and comprises volcanic breccias, andesite and basalt flows, tuffs, lapilli tuffs, pumiceous tuffs, volcanoclastic sandstones, mudstones, and intercalated limestones (Clements, 2007). The Jampang Formation makes up much of the Southern Mountains region, extends from Cileteuh to Pangandaran, and has an estimated thickness of as much as 5 km (Clements, 2007). This formation comprises two parts, i.e., the lower and upper parts. The lower part consists of marl, sandstone, and calcareous brecciated tuff of andesitic and dacitic composition with intercalation of limestone beds. The upper part consists of volcanic breccia and tuff, and locally contains nodules and lenses of limestone with andesitic to dacitic sills, dikes, stocks, and quartz veins (Sukanto, 1975). Based on the previous research and field study, only the Tertiary volcanic rocks and alluvial deposit that exposed to the surface, whereas the limestone and the intrusions are poorly exposed (Wu *et al.*, 2015; Zhang *et al.*, 2015).

The research area's regional structure (Figure 1B) consists of two main trends, i.e., NW-SE and NE-SW, called the Sumatra and the Meratus trends (Yulianto, 2007; Zhang *et al.*, 2015). The NW-SE trending fault around the research area has a striking angle between 310-320°, whereas the NE-SW trending fault has a striking angle between 45-50° (Zhang *et al.*, 2015).

3 METHODOLOGY

Besides field work and geological mapping data, this research uses three (3) laboratory methods, i.e., petrography, ore microscopy, and atomic absorption spectrometry (AAS). A total of 6 thin sections of skarn samples and 5 polished sections of ore from 5 boreholes (Figure 2A) were prepared at Obsidian Laboratory, Bandung. The petrography and ore microscopy analyses were conducted using Euromex BS.1053-PLMi polarizing microscope at the Department of Geological Engineering, Universitas Gadjah Mada. Petrography and ore microscopy were used to identify and characterize minerals and ores of the skarn deposit with the main goal of interpreting the mineral paragenesis. The mineral abundance is interpreted based on the visual abundance

standard by Terry & Chilingar (1955) with proportions classification from Morrison (1997). AAS data of 15 samples from 3 boreholes were obtained from PT. Generasi Muda Bersatu. The AAS method is conducted with PerkinElmer's PinAAcle 500 Flame Atomic Absorption Spectrometer in PT. Generasi Muda Bersatu's internal laboratory to quantify the deposit's Pb, Zn, and Cu grades.

4 RESULTS AND DISCUSSION

4.1 Geology of Kujang skarn deposit

Based on field study and geological mapping data, the geology in the research area consists of dacite porphyry, tuff breccia, lapilli tuff, and limestone (Figure 2A). The volcanic rocks (i.e., tuff breccia and lapilli tuff) and dacite porphyry are exposed on the surface, while the limestone is only in the mine pit. Stratigraphically, the volcanic rocks were placed on top of the limestone and then intruded by the dacite porphyry. The volcanic rocks have been strongly altered to form propylitic and argillic alterations, whereas the limestone exposed in the mine pit has been altered to marble caused by the metamorphism process (Figure 2D). The skarn ore body is found at the contact between marble and volcanic rocks (Figure 2B).

The dacite porphyry, as the ore-causative intrusion, is only found as floats and boulders (Figure 2C) on the east side of the pit. No dacite outcrop has been found in the research area because it has already been altered and weathered to clay, with only the quartz relic remaining. The dacite is light grey with quartz, hornblende, and plagioclase phenocryst crystals. There are four structural trends in the research area: NW-SE, N-S, E-W, and NE-SW (Figure 2A). The NW-SE trend is expressed with three dextral strike-slip faults, N-S with two sinistral strike-slip faults, NE-SW with a dextral strike-slip fault, and E-W with five normal faults.

4.2 Skarn alteration minerals characteristics

Skarn mineralogy by other authors such as Dana *et al.* (2022), Furqan (2014), and Idrus *et al.* (2011) can be divided into prograde and retrograde stage alteration minerals. The term prograde alteration refers to an alteration

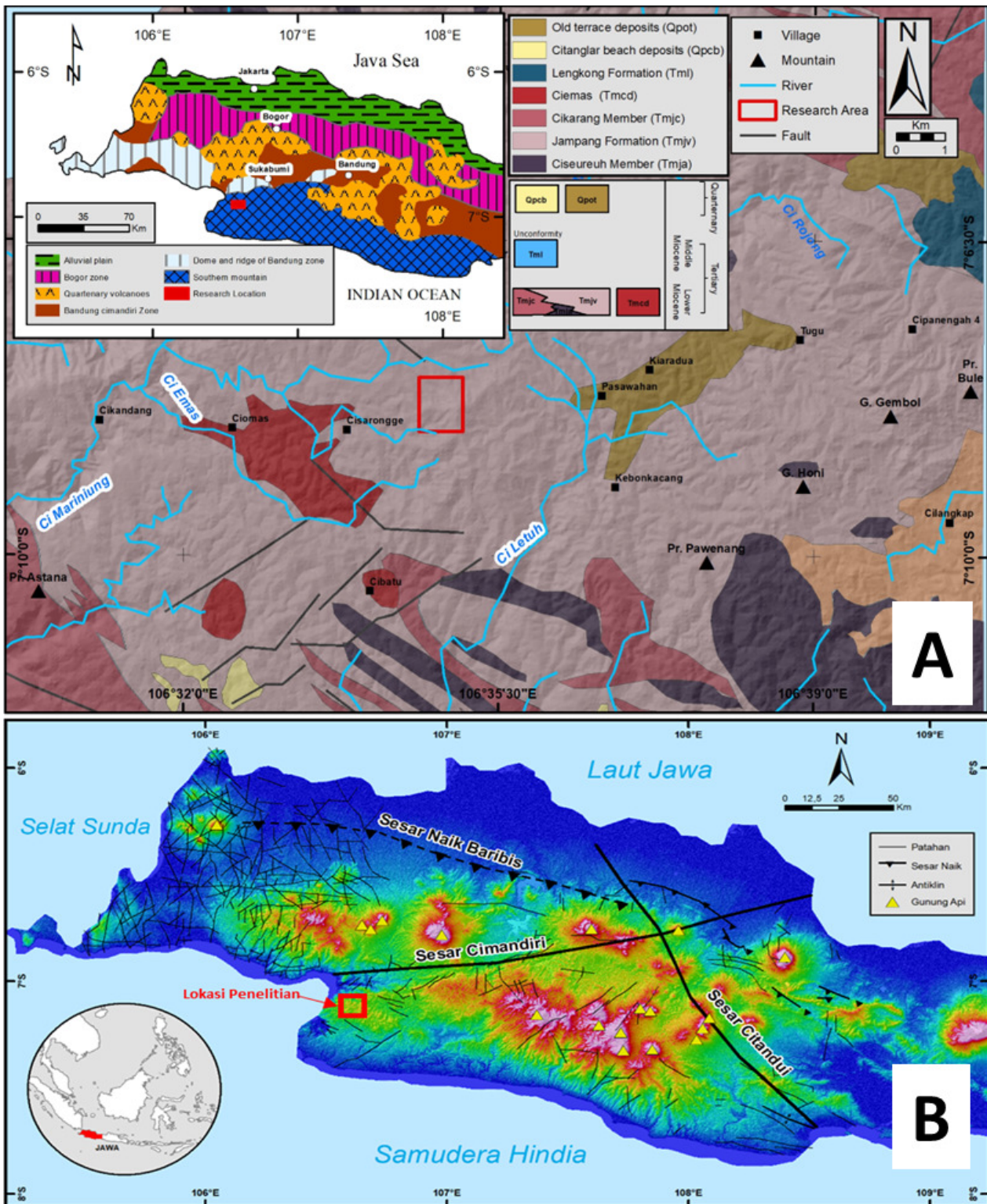


FIGURE 1. (A) A regional geology map of the research area (modified after Sukamto, 1975; fault location compiled after Zhang *et al.*, 2015) was added with the physiography map of West Java (modified after van Bemmelen, 1949); (B) West Java's regional structure map taken and modified from Yulianto (2007).

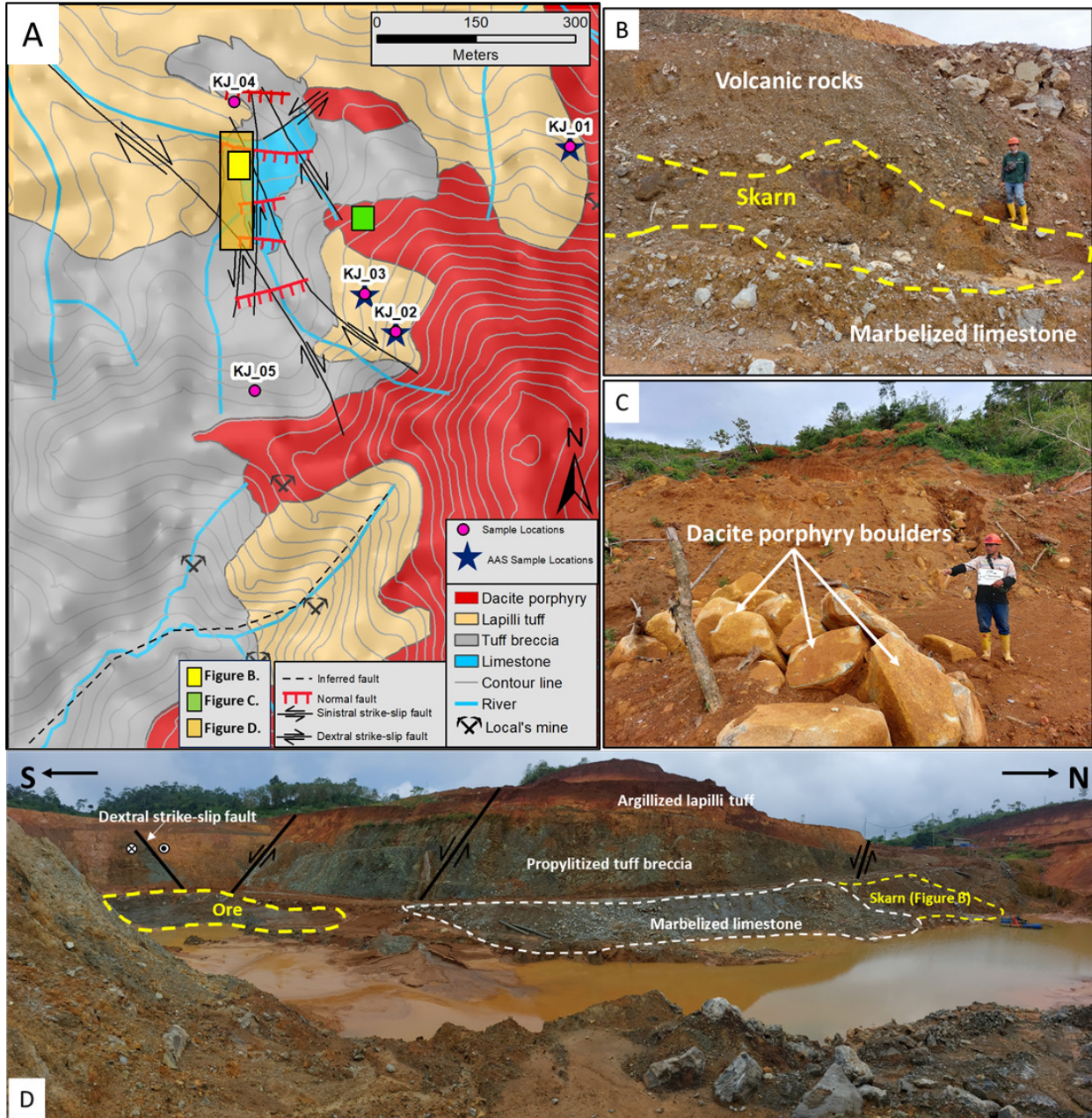


FIGURE 2. (A). Detailed geological map of the research area with undisclosed coordinates; (B). Skarn is found along the contact between marbelized limestone and volcanic rocks; (C). Dacite porphyry was found as floats and boulders at the pit area; (D) Mine pit photo of the Kujang Pb-Zn skarn, showing the overall geological condition of the deposit.

stage characterized by high-temperature anhydrous minerals, especially garnet and clinopyroxene. At the same time, retrograde alteration refers to lower-temperature hydrous minerals such as chlorite and epidote that can overprint and obliterate the prograde alteration mineral (Meinert, 2020).

At the Kujang Prospect skarn, the prograde minerals that have been found comprise garnet, clinopyroxene, wollastonite, and vesuvianite. Garnets in the Kujang Prospect skarn are the rarest prograde mineral with an abundance of <1% and are found in the skarn as hard, brown, fine-grained crystals. Under the microscope, garnets show pale green with high relief under PPL and black interference color under XPL. Garnets also show typical zoning texture (Figure 3A). The most abundant prograde mineral, clinopyroxene, presents greenish fine-grained crystals that are often difficult to distinguish megascopically from chlorite and epidote. On the microscopic scale, clinopyroxene presents as disseminated prismatic euhedral to subhedral crystals with second-order varied interference colors, commonly from blue to red (Figure 3B). Wollastonite is found as dark green with a dull luster megascopically, whereas, under XPL, this mineral has a distinguish fibrous habit with first-order light-dark brown interference color. The last prograde mineral that has been found is vesuvianite. This mineral is found growing together with wollastonite (Figure 3C) and has a first-order light-dark grey interference color, whereas this mineral cannot be identified megascopically.

The retrograde alteration is characterized by chlorite, epidote, calcite, alunite, quartz, and actinolite. Chlorite (Figure 3E) and epidote (Figure 3D) are the most abundant retrograde minerals. Both exhibit greenish fine-grained crystals and are difficult to distinguish on a megascopic scale but show different optical properties under the microscope. Calcite, chlorite, and epidote are retrograde minerals found to replace clinopyroxene (Figure 3B). Actinolite, which belongs to the amphibole group, shows prismatic subhedral crystals with brown, yellow, and grey interference colors (Figure 3F). Like the other retrograde minerals, actinolite tends to be a replacement product of clinopyroxene. Actinolite exhibits a thin, needle-like,

randomly oriented crystal with green, yellow, and brown first-order interference color on a microscopic scale.

4.3 Ore minerals characteristics

From the ore microscopy analysis of five ore samples, metalliferous and ore minerals of the Kujang Prospect skarn consist of sphalerite (ZnS), galena (PbS), pyrrhotite (Fe_{1-x}S), chalcopyrite (CuFeS_2), and pyrite (FeS_2). Sphalerite is the most common ore mineral within the ore body. Sphalerite is grey with low reflectance under plane-polarized light (PPL). This mineral ranges from 0.1 to >1 mm with a subhedral-anhedral crystal shape (Figure 4A-D). Galena is the second most abundant ore mineral after sphalerite. This mineral shows a special and unique texture called the triangular pit, a subhedral-anhedral shape with a high reflectance light grey color under PPL (Figure 4C-D).

Chalcopyrite is the rarest mineral found in ore bodies and is strongly associated with sphalerite. Chalcopyrite is found to replace sphalerite and, as an inclusion within sphalerite, is known as chalcopyrite disease (Figure 4C). Under PPL, chalcopyrite is subhedral-anhedral with a distinct low reflectance brassy yellow color. Pyrrhotite within the orebodies is sometimes difficult to distinguish from pyrite (Figure 4F). This iron sulfide mineral has a strong anisotropic with a reddish-brown interference color that distinguishes this mineral from pyrite. Pyrrhotite and pyrite may form a massive ore body in the Kujang prospect. Pyrite, a sulfide mineral that is common but not economically significant, is found in the form of euhedral cubic to subhedral crystals and found along other sulfide minerals such as galena, sphalerite, and pyrrhotite. Pyrite found to replace both galena and sphalerite, suggests has board deposition temperature and stable condition.

4.4 Atomic Absorption Spectrometry (AAS)

Based on AAS data from the 15 ores sample (Table 1), the Kujang Prospect has an average grade of 2.06 % Pb with a minimum grade of 0.01% and a maximum grade of 8.77 %. The Zn grade is consistent with the abundance of sphalerite as the main Zn-bearing mineral has a

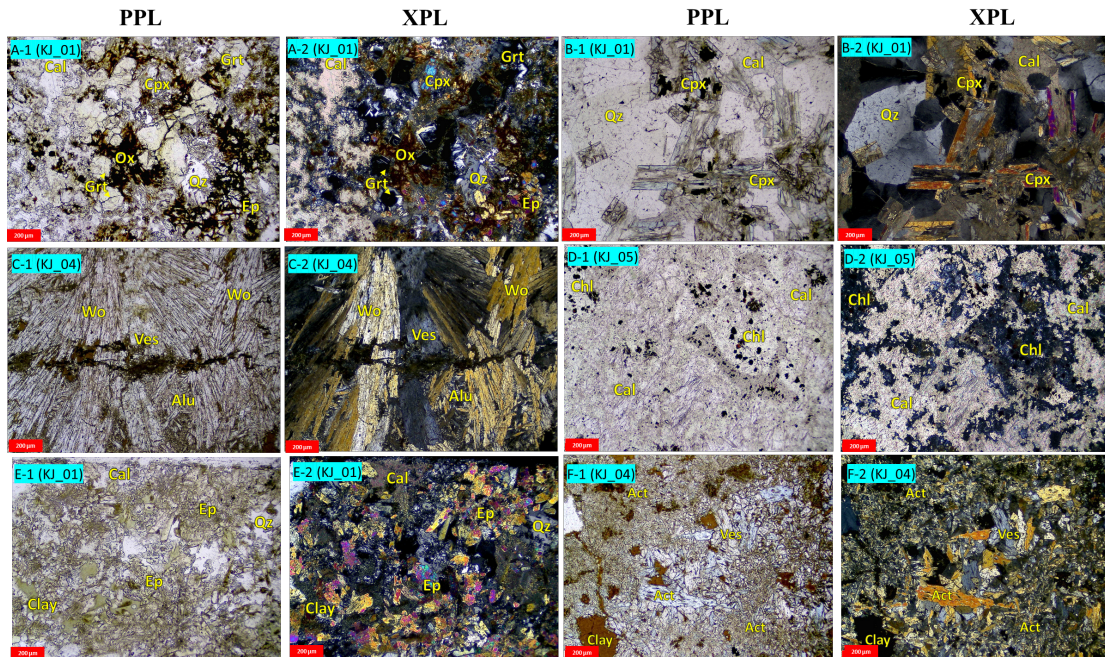


FIGURE 3. Photomicrograph of skarn mineral assemblages, code-1 in PPL and code-2 in XPL, all picture scale at $200\mu\text{m}$ (A). garnet and clinopyroxene as prograde minerals overprinted by quartz, calcite, and epidote; (B). coarse-grained clinopyroxene altered to calcite and surrounded by quartz; (C). fibrous wollastonite and vesuvianite; (D). epidote associated with calcite and clay as retrograde alteration mineral (E) calcite associated with chlorite; (F). prismatic actinolite crystals surrounded by alunite. Grt = garnet; Cpx = clinopyroxene; Wo = wollastonite; Ep = epidote; Chl = chlorite; Ves = vesuvianite; Cal = calcite; Act = actinolite; Ox = Fe-oxide.

minimum grade of 0.08 %, a maximum grade of 19.75 % with an average grade of 6.45 % and Cu has an average grade of 1.81 %. Few amounts of Ag have been found on average of 41.63 ppm.

4.5 Discussion

Lithology and geological structure are the two aspects that control the Kujang Prospect skarn formation. The skarn is formed because the limestone-rich with Ca undergoes the metasomatism process, while the limestone itself also acts as the main host for skarn mineralization. As stated, the skarn ore body is found at the contact between marbleized limestone and volcanic rocks, while dacite porphyry is interpreted as the ore-causative intrusion. The dacite porphyry is the only intrusive rock that can be found during the exploration drilling program until now. In terms of structural aspect, the NW-SE trend, expressed with three right-lateral strike-slip faults, acts as the pathway for the mineralizing fluids. This conclusion is derived from the ore bodies being found along this fault.

The mineral paragenesis of the Kujang skarn

deposit can be divided into 2 main groups, i.e., prograde and retrograde, as seen in Figure 5 below. Prograde minerals such as garnet, clinopyroxene, wollastonite, and vesuvianite are assumed to be formed at more than 300°C (Idrus *et al.*, 2011). At the lower temperature, between $150\text{--}300^{\circ}\text{C}$, minerals that belong to the retrograde group, such as epidote, chlorite, calcite, and actinolite, were formed and replaced the earlier prograde anhydrous minerals (Idrus *et al.*, 2011). Quartz and pyrite interpreted can be formed at both prograde and retrograde. The ore mineralization process mainly occurs during the early retrograde stage, such as at Erstberg (Meinert *et al.*, 1996) and Ruwai (Idrus *et al.*, 2011). Specifically, as stated in Kwak (1986), Pb-Zn skarns have an economic mineralization temperature of $250\text{--}320^{\circ}\text{C}$. Similar to Ruwai, no Ag sulfide mineral is identified in the analyzed sample. It can be interpreted that the few Ag content in the deposit came from galena as an Ag-bearing mineral (Idrus *et al.*, 2011). Based on observation of ore microscopy, sphalerite and galena are the most abundant and major eco-

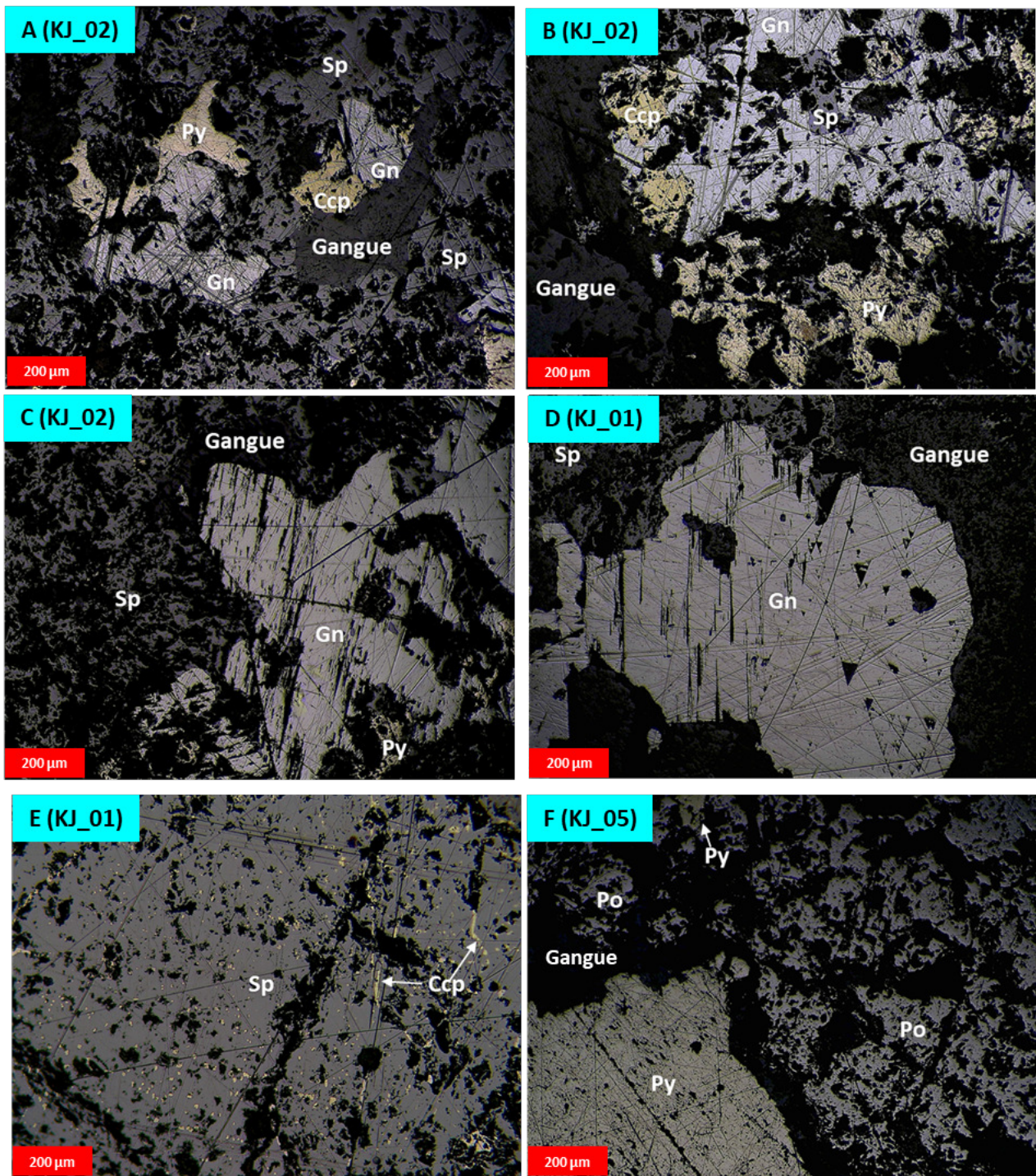


FIGURE 4. Photomicrograph of ore minerals, all photos in PPL, all picture scale at 200 μ m (A-B). Sphalerite presents along with galena, pyrite, and chalcopyrite (B-C). With a unique triangular pit texture, Galena presents with sphalerite (E). Chalcopyrite as inclusion in sphalerite as chalcopyrite disease; (F). Euhedral pyrite presents with pyrrhotite. Sp = sphalerite; Gn = galena; Ccp = chalcopyrite; Py = pyrite; Po = pyrrhotite.

TABLE 1. The resume of AAS data shows the Pb, Zn, Cu, and Ag grades of the skarn deposit. PT conducts this AAS measurement. Generasi Muda Bersatu (GMB).

Borehole	Number of Sample	Data Summary	Grade (wt.%, except for Ag in ppm)			
			Pb	Zn	Cu	Ag
KJ_1	6	min	0.03	1.13	0.14	13.13
		max	6.90	19.75	24.43	164.55
		average	1.44	9.23	4.29	59.35
KJ_2	5	min	0.05	0.08	0.03	5.03
		max	8.77	7.72	0.18	69.73
		average	4.39	4.38	0.12	42.76
KJ_3	4	min	0.01	0.12	0.14	1.33
		max	0.19	0.12	0.27	33.03
		average	0.08	0.12	0.22	13.64
All Data	15	min	0.01	0.08	0.03	1.33
		max	8.77	19.75	24.53	164.55
		average	2.06	6.45	1.81	41.63

nomic ore minerals found in the Kujang Skarn. That fact aligns with the result of AAS, where the skarn has an average grade of 2.06 % Pb and 6.45 % Zn. Based on these 2 findings, the Kujang skarn can be categorized as a Pb-Zn skarn.

A geophysical method such as detailed geomagnetic is recommended for further exploration programs. The mineralized and intrusion zones can be identified and separated from the geomagnetic data. Delineated the intrusion zone is critical because, theoretically, the ore bodies do not form near the intrusion. The geological structures not exposed on the surface can be recognized from the geomagnetic anomaly so that the exploration drilling activity can be focused along the geomagnetic's interpreted structure. Mineral chemistry can be conducted to precisely know the exact end member of the skarn's calc-silicate mineral, whereas detailed ore chemistry can be used to reveal the potential rare element carried by the metalliferous and ore minerals.

5 CONCLUSION

Lithology and geological structure are the main aspects controlling the formation of the Kujang skarn prospect. The skarn mineralization is mainly hosted by limestone and deposited on the contact between volcanic rocks and marbleized limestone. The dacite porphyry is interpreted to be the ore-causative intrusion. Three right-lateral strike-slip faults with an NW-SE

trend act as structural control because the ore bodies are found along this fault. Skarn alteration minerals can be divided into 2 main groups, i.e., prograde and retrograde. The prograde skarn is characterized by garnet, clinopyroxene, wollastonite, and vesuvianite, whereas the retrograde mineral is typified by epidote, chlorite, calcite, and actinolite. Based on ore mineral type and assay data, this skarn can be identified as Pb-Zn skarn, which is economically significant with an average grade of 2.06 % Pb, 6.45 % Zn, and 1.81 % Cu.

Acknowledgements The authors would like to thank the management and geologists of PT. Generasi Muda Bersatu, for the assistance during fieldwork and publication permission, and the AAS data and core samples for analysis. I thank the Geological Engineering Department, Universitas Gadjah Mada, for the opportunity to conduct petrography and ore microscopy analysis.

REFERENCES

- Al Furqan, R. (2014). Geology of Pinang-Pinang Skarn Au-Cu ± Mo Deposit, Aceh, Indonesia. *Proceedings of Sundaland Resources-MGEEI Annual Convention*, 291–299.
- Bensaman, B., Furqan, R. A., Rosana, M. F., & Yuningsih, E. T. (2015). Hydrothermal Alteration and Mineralization Characteristics of Gajah Tidur Prospect, Ertsberg Mining District, Papua, Indonesia. *Proceedings of the 2nd International Conference and 1st Joint Conference Faculty of Geology Uni-*

- versitas Padjajaran with Faculty of Science and Natural Resources University of Malaysia Sabah*, 1–9.
- Clements, B. (2007). Cretaceous to Late Miocene stratigraphic and tectonic evolution of West Java. Indonesian Petroleum Association, *Proceedings 31st Annual Convention*, 87–104. <https://doi.org/10.29118/IPA.1520.07.G.037>
- Dana, C. D. P., Agangi, A., Takahashi, R., Idrus, A., Lai, C., & Nainggolan, N. A. (2022). Element mobility during formation of the Ruwai Zn-Pb-Ag skarn deposit, Central Borneo, Indonesia. *Resource Geology*, 72(1), 1–25. <https://doi.org/10.1111/rge.12290>
- Idrus, A., Setijadji, L. D., & Fenny, T. (2011). Geology and Characteristics of Pb-Zn-Cu-Ag Skarn Deposit at Ruwai, Lamandau Regency, Central Kalimantan. *Jurnal Geologi Indonesia*, 6(4), Article 4.
- Kwak, T. A. P. (1986). Fluid inclusions in skarns (carbonate replacement deposits). *Journal of Metamorphic Geology*, 4(4), 363–384. <https://doi.org/10.1111/j.1525-1314.1986.tb00358.x>
- Meinert, L. D. (2020). Geology, Policy, and Wine – The Intersection of Science and Life. *Geochemical Perspectives*, 9(1), Article 1. <https://doi.org/10.7185/geochempersp.9.1>
- Meinert, L. D., Hefton, K. K., Mayes, D., & Tasiran, I. (1996). Geology, Zonation, and Fluid Evolution of the Big Gossan Cu-Au Skarn Deposit, Ertsberg District, Irian Jaya. *Economic Geology*, 92(5), 509–534. <https://doi.org/10.2113/gsecongeo.92.5.509>
- Morrison, K. (1997). *Important Hydrothermal Minerals and Their Significance* (7th ed.). Kingston Morrison Limited.
- Sukamto, R. (1975). *Peta Geologi Lembar Jampang Balekambang [Map]*. Pusat Penelitian dan Pengembangan Geologi.
- Terry, R. D., & Chilingar, G. V. (1955). Summary of “Concerning some additional aids in studying sedimentary formations,” by M. S. Shvetsov. *Journal of Sedimentary Research*, 25(3), 229–234. <https://doi.org/10.1306/74D70466-2B21-11D7-8648000102C1865D>
- van Bemmelen, R. W. (1949). *The geology of Indonesia*. (Vol. 1). The Hague.
- Wu, C.-Q., Zhang, Z.-W., Zheng, C.-F., & Yao, J.-H. (2015). Mid-Miocene (~17 Ma) quartz diorite porphyry in Ciemas, West Java, Indonesia, and its geological significance. *International Geology Review*, 57(9–10), Article 9–10. <https://doi.org/10.1080/00206814.2014.908748>
- Xu, R., Deng, M.-G., Li, W.-C., Lai, C.-K., Zaw, K., Gao, Z.-W., Chen, Y.-H., Niu, C.-H., & Liang, G. (2021). Origin of the giant Luziyuan Zn-Pb-Fe(-Cu) distal skarn deposit, Baoshan block, SE Tibet: Constraints from Pb-Sr isotopes, calcite C-O isotopes, trace elements, and Sm-Nd dating. *Journal of Asian Earth Sciences*, 205, 104587. <https://doi.org/10.1016/j.jseae.2020.104587>
- Yulianto, I. (2007, May 1). Structural and stratigraphic evolution of the offshore Malingping Block, West Java, Indonesia. *Proc. Indon Petrol. Assoc., 31st Ann. Conv. Thirty-First Annual Convention*. <https://doi.org/10.29118/IPA.2540.07.G.036>
- Zhang, Z., Wu, C., Yang, X., Zheng, C., & Yao, J. (2015). The trinity pattern of Au deposits with porphyry, quartz-sulfide vein, and structurally-controlled alteration rocks in Ciemas, West Java, Indonesia. *Ore Geology Reviews*, 64, 152–171. <https://doi.org/10.1016/j.oregeorev.2014.07.003>